

Supporting Information

# Self-Forming Norbornene-Tetrazine Hydrogels with Independently Tunable Properties

Kirstene A. Gultian<sup>1</sup>, Roshni Gandhi<sup>1</sup>, Tae Won B. Kim<sup>2</sup>, Sebastián L. Vega<sup>1\*</sup>

<sup>1</sup>Department of Biomedical Engineering, Rowan University, Glassboro NJ 08028, USA

<sup>2</sup>Department of Orthopaedic Surgery, Cooper Medical School of Rowan University, Camden NJ 08103

\*Corresponding author

Sebastián L. Vega, Ph.D: vegas@rowan.edu

## SUPPORTING INFORMATION

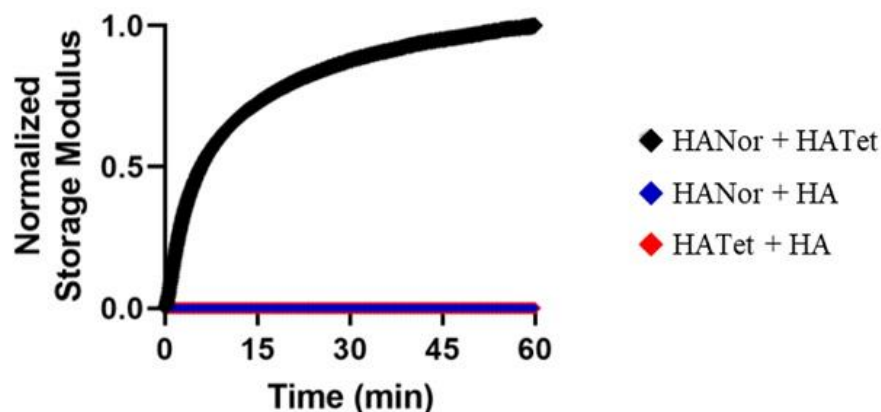


**Figure S1.** Storage modulus ( $G'$ ) evolution through time sweep rheometry for 2% w/v Nor-Tet hydrogels normalized to plateau  $G'$  of the HANor + HATet group (black diamond). Mixing of HANor with unmodified HA (blue diamond) or HATet with unmodified HA (red diamond) does not result in crosslinking.

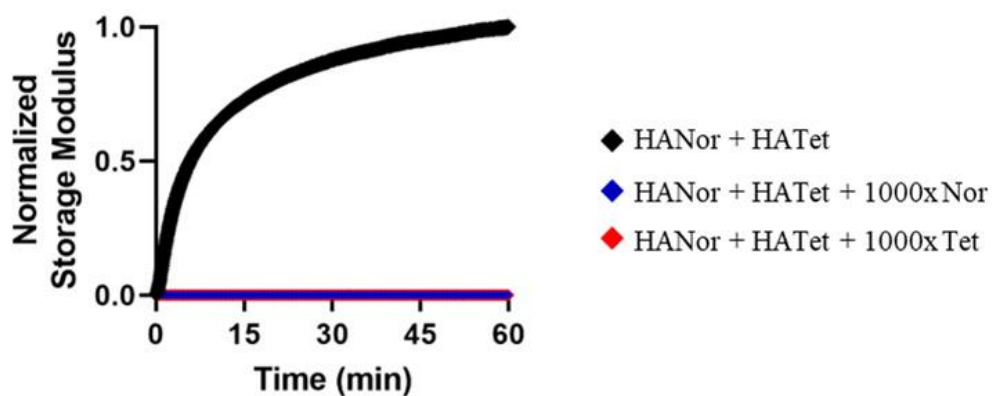


**Figure S2.** Storage modulus ( $G'$ ) evolution through time sweep rheometry for 2% w/v Nor-Tet hydrogels normalized to plateau  $G'$  of the HANor + HATet group (black diamond). Addition of free Nor (blue diamond) or Tet (red diamond) molecules (1000x molar excess) to the mixture abrogates HANor crosslinking with HATet. 1,000x molar excess of free Nor is equivalent to 2.5 mM Nor-NH<sub>2</sub>. 1,000x molar excess of free Tet is equivalent to 1.6 mM Tet-NH<sub>2</sub>.

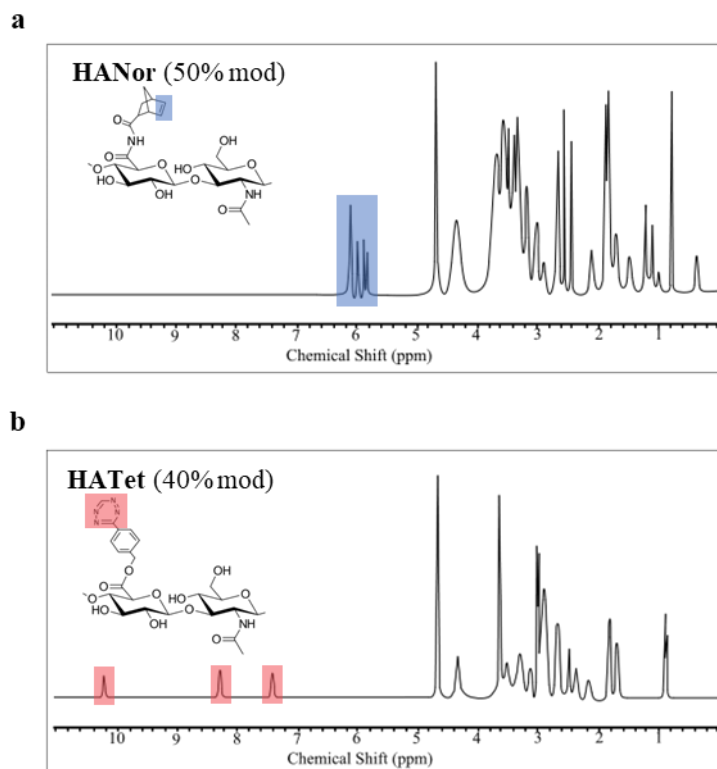


**Figure S3.** <sup>1</sup>H NMR spectra of (a) HANor and (b) HATet.

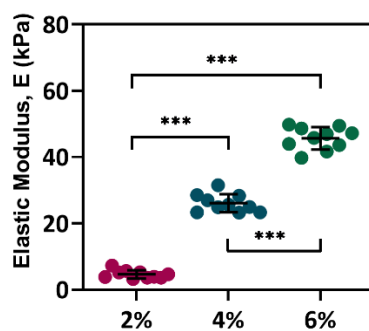


**Figure S4.** Elastic moduli of 2%, 4%, and 6% w/v Nor-Tet hydrogels. Values were determined using compression mechanical testing. Scatter dot plot shown as mean  $\pm$  SD ( $n \geq 6$  samples per condition) with significant differences determined with ANOVA followed by Tukey's post hoc test where \*\*\* $p < 0.001$ .

**Table S1.** Diene and dienophiles used in Diels-Alder reactions with corresponding storage moduli ( $G'$ ) and gelation times.

Diene	Dienophile	Storage modulus, $G'$	Gelation time	Reference
Furan	Di-Maleimide	< 1,000 Pa	120 – 180 min	25
Methylfuran	Di-Maleimide	< 1,500 Pa	15 min	26
Furan	Maleimide	5,000 – 35,000 Pa	15 – 170 min	27
Fulvene	Maleimide	< 1,000 Pa	6 – 35 min	28
Tetrazine	Di-Norbornene	< 2,500 Pa	< 10 min	29
Tetrazine	Norbornene	< 500 Pa	100 min	30
Tetrazine	Norbornene	< 4,500 Pa	< 15 min	31

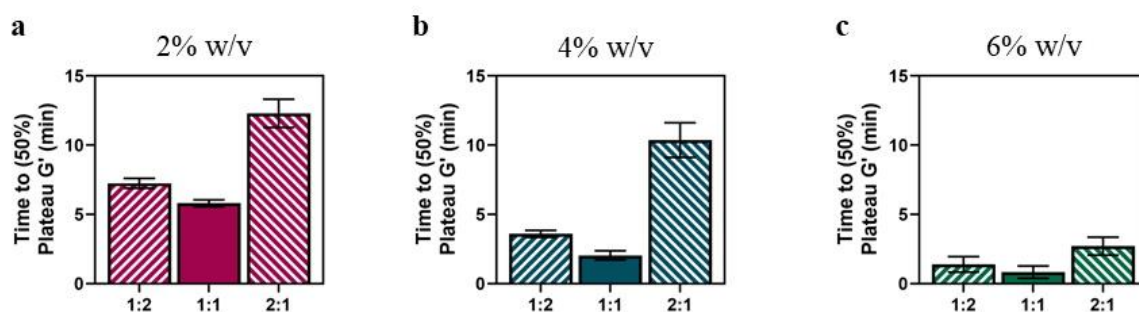


**Figure S5.** Physical characterization of Nor-Tet hydrogels at 37 °C. Time to 50% plateau  $G'$  of (a) 2%, (b) 4%, and (c) 6% w/v Nor-Tet hydrogels at 1:2, 1:1, and 2:1 HANor:HATet stoichiometric ratios. Bar graphs shown as mean  $\pm$  SD ( $n \geq 3$  samples per condition).

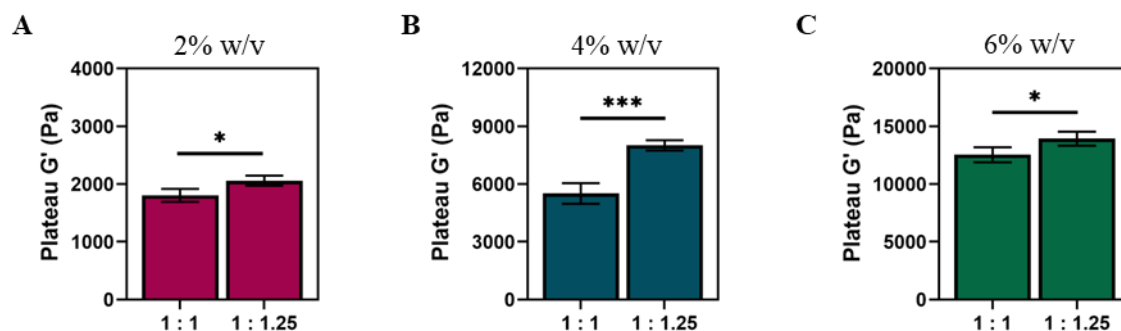


**Figure S6.** Physical characterization of Nor-Tet hydrogels at 37 °C. Plateau  $G'$  of (a) 2%, (b) 4%, and (c) 6% w/v Nor-Tet hydrogels at 1:1 and 1:1.25 HANor:HATet stoichiometric ratios. Bar graphs shown as mean  $\pm$  SD ( $n \geq 3$  samples per condition) with significant differences determined with ANOVA followed by Tukey's post hoc test where \* $p < 0.05$ , \*\*\* $p < 0.001$ .

**Table S2.** Reaction parameters to create HANor(Pep+) macromers with appropriate cRGD (Sequence: GCGYGRGDSPG; MW: 1,025 g mol<sup>-1</sup>) concentrations to achieve an effective concentration of 2 mM.

Macromer w/v	HANorMe (mg)	cRGD (mg)
2%	100	20.5
4%	100	10.3
6%	100	6.9

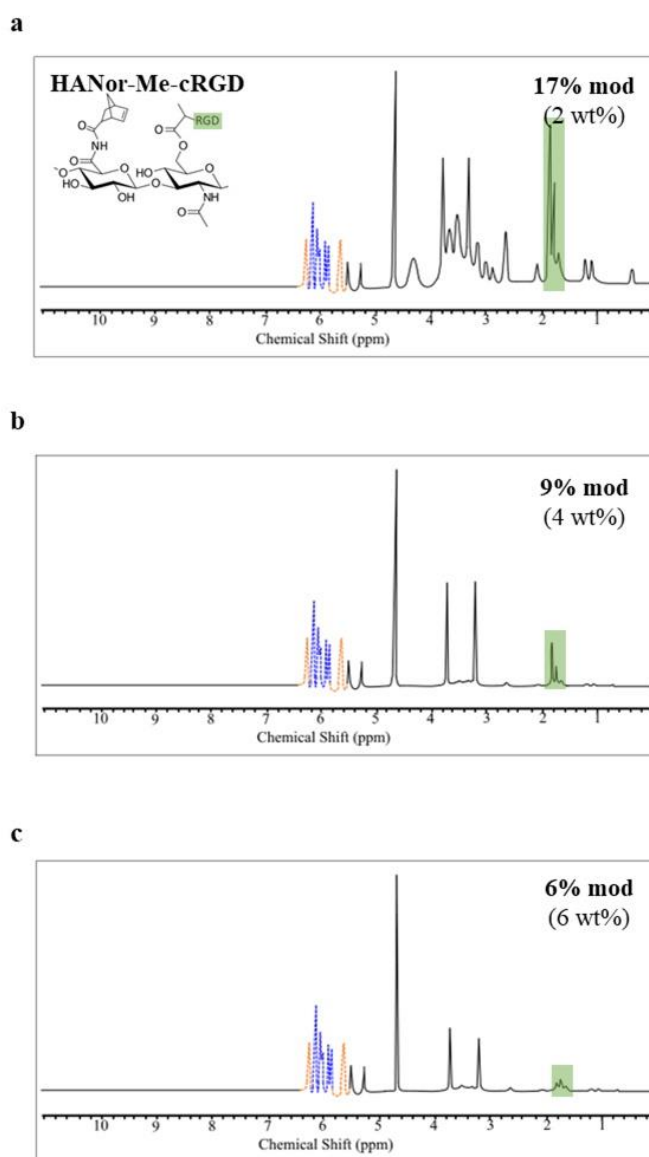


**Figure S7.** <sup>1</sup>H NMR spectra of HANor(cRGD+). Distinct peaks for cRGD peptides are seen, and these peaks decrease with increasing Nor-Tet w/v. <sup>1</sup>H NMR spectra for HANor(cRGD+) used to form (a) 2%, (b) 4%, and (c) 6% w/v Nor-Tet hydrogels.

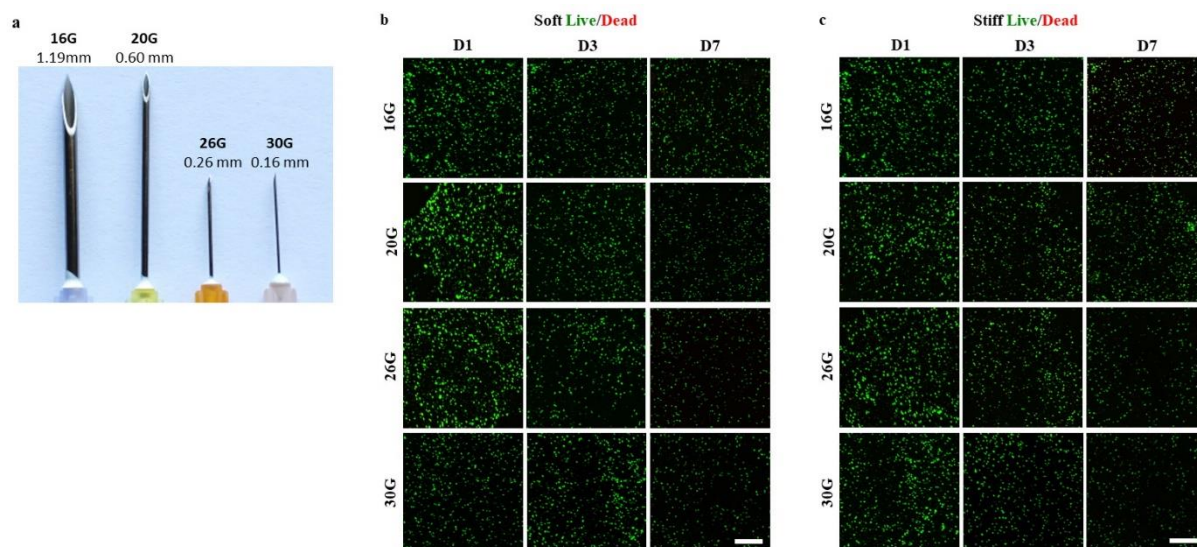


**Figure S8.** 3D viability of MSCs injected through different size syringe needles. (a) Needles used for extrusion have internal diameters ranging from 0.16 to 1.19 mm. Representative live (green) and dead (red) staining of MSCs extruded through different needle sizes for (b) Soft (2% w/v) and (c) Stiff (6% w/v) Nor-Tet hydrogels. Scale bars: 500  $\mu\text{m}$ .

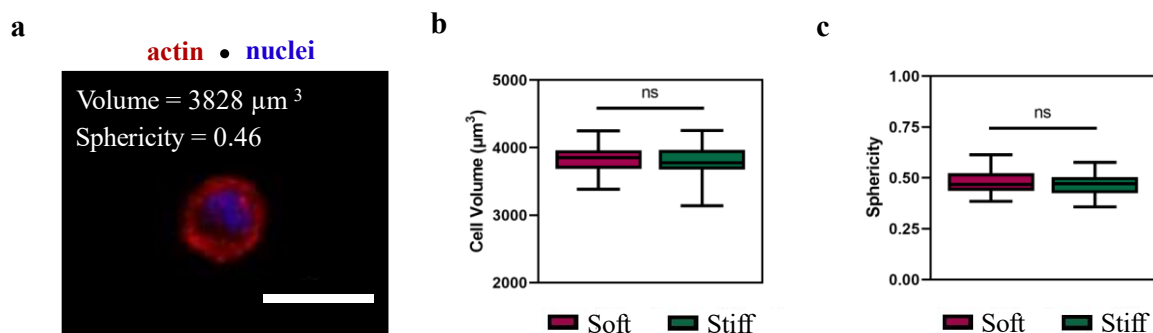


**Figure S9.** 3D morphology of MSCs encapsulated in Soft (2% w/v) and Stiff (6% w/v) Nor-Tet hydrogels. (a) Representative F-actin (red) and nuclear (blue) staining of an MSC encapsulated in Nor-Tet hydrogels (2% w/v shown). Quantification of (b) Volume and (c) Sphericity of MSCs in Soft and Stiff Nor-Tet hydrogels. Bar graphs shown as mean  $\pm$  SD ( $n \geq 3$  samples per condition) with no significant differences (ns) determined with ANOVA. Scale bar: 50  $\mu\text{m}$ .

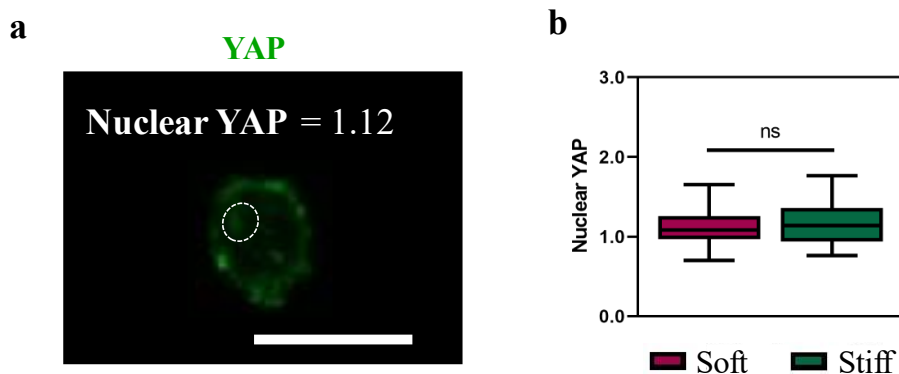


**Figure S10.** 3D matrix mechanosensing of MSCs encapsulated in Soft (2% w/v) and Stiff (6% w/v) Nor-Tet hydrogels. (a) Representative image of an MSC encapsulated in a Soft Nor-Tet hydrogel stained for YAP (*green*). (b) Nuclear YAP quantification of MSCs on Soft and Stiff Nor-Tet hydrogels stained for YAP. Bar graphs shown as mean  $\pm$  SD ( $n \geq 3$  samples per condition) with no significant differences (ns) determined with ANOVA. Scale bar: 50  $\mu$ m.

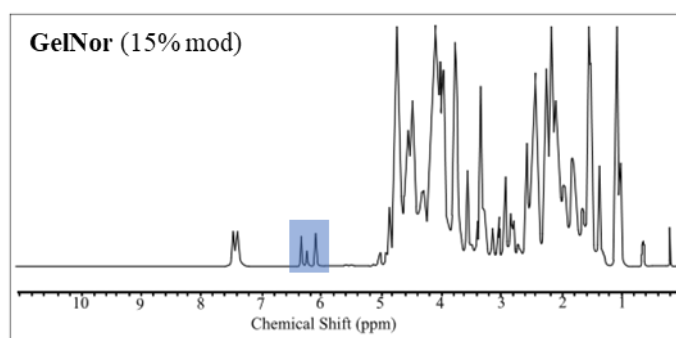


**Figure S11.**  $^1\text{H}$  NMR spectra of GelNor.